Seventeenth International Conference on
Geometry, Integrability and Quantization
June 5–10, 2015, Varna, Bulgaria
Ivaïlo M. Mladenov, Guowu Meng
and Akira Yoshioka, Editors
Avangard Prima, Sofia 2016, pp 182–195
doi: 10.7546/giq-17-2016-182-195

CURVATURE EFFECTS IN 1-D AND 2-D JOSEPHSON JUNCTIONS

TOMASZ DOBROWOLSKI

Institute of Physics UP, 30-084 Cracow, Poland

Abstract. The gauge invariant phase difference between superconducting electrodes is a dominating dynamical degree of freedom in the Josephson junction. This rapport concerns the influence of the curvature of the junction on the dynamic of this field variable. The effects of curvature are discussed in the long and large area junctions. In particular the dynamics of the fluxion and the kink front are studied.

MSC: 53Z05, 35L70,53A04,53A05
Keywords: Fluxion, Josephson junction, sine-Gordon

1. Introduction

The Josephson junction is a device that consists of two superconducting electrodes separated by a very thin layer of insulator or other material. For example, in the case of a dielectric barrier this thickness is in the range 10-20 Å. The leading effect that determines the operation of this device is tunnelling of Cooper pairs from one to the other electrode. The effect was first predicted by Josephson [17] and then observed experimentally by Anderson and Rowell [2]. As far as the dimension of the junction is considered we can classify the junctions in the following way

- Large area Josephson junction, which is two dimensional system.
- If one of the transverse dimensions is smaller than the Josephson length then there is no dynamics in this direction and we have one dimensional system.
- If both transverse dimensions are smaller than the Josephson penetration depth than we have zero dimensional system called point contact.

The analysis of this system can be performed on the background of the Maxwell equations with Landau-Ginzburg current of Cooper pairs. In case of superconducting electrodes we also use the Londons equation that relates the electric field with

time change of the current. Each of the superconducting electrodes is described by the many-particle wave function. The modulus of this function describes the square root of density of Cooper pairs in the superconducting electrode. Inside the superconductor (in the low energy regime) density of Cooper pairs is almost constant. The same situation we have in both (top and bottom) electrodes. Because the thickness of the dielectric layer is very small those two electrodes are not independent quantum systems. In the low energy regime the only nontrivial dynamical variable that describes the system is the gauge invariant phase difference ϕ. This quantity is a measure of the magnetic flux. The outcome of these considerations is the nonlinear wave equation that describes the dynamics of the field ϕ. This equation has the form of the sine-Gordon equation [5], [28]. The properties and applications of this model are described in many texts [1, 14, 16, 23, 24, 30]. The properties of the Josephson junction are modified in the curved junctions. The studies concern constant and also position dependent curvatures [12, 13]. For example, in case of quickly varying curvatures this equation takes the form

$$\frac{1}{\bar{c}^2}\,\partial_t^2\phi + \frac{\gamma}{\bar{c}}\,\partial_t\phi + \frac{\beta}{\bar{c}}\,\cos\phi\;\partial_t\phi - \partial_s^2\left(\mathcal{F}\,\phi\right) + \frac{1}{\lambda_J^2}\,\sin\phi = I_b. \tag{1}$$

Here λ_J is Josephson penetration depth, which tells how much the magnetic field penetrates the junction

$$\lambda_J = \sqrt{\frac{\hbar c^2}{8\pi e \lambda J_0}} \tag{2}$$

and $\bar{c}$ is Swihart velocity, which determines the maximal speed of propagation of electromagnetic excitations in the junction

$$\bar{c} = \frac{c}{\sqrt{4\pi\lambda C}}. \tag{3}$$

According to the standard notation $\hbar$ is the Dirac constant, e is the elementary charge, c is speed of the light in vacuum, J_0 is critical Josephson current, C is capacitance per unit area and $\lambda = 2\lambda_L + w$, where λ_L is Londons penetration depth and w is a width of the dielectric layer. Additionally

$$\gamma = \frac{\sigma_0}{\bar{c}\,C}, \qquad \beta = \frac{\sigma_1}{\bar{c}\,C} \tag{4}$$

where σ_0 and σ_1 are appropriate conductivities of the junction. The first conductivity is connected with the quasiparticle tunnelling current and the second describes a quasiparticle pairs interface current. Usually, the constant γ is small quantity and β is even smaller and therefore they are commonly neglected. The second term in the equation 1 is responsible for the dissipation in the system. The curvature effects are described by the function

$$\mathcal{F} = \frac{1}{aK(s)} \ln\left(\frac{2 + aK(s)}{2 - aK(s)}\right) \tag{5}$$

where $K(s)$ is a curvature of the junction identified with the curvature of the curve located in the center of the dielectric layer. Moreover, the quantity I_b describes the externally controlled, by the experimentalist, bias current.

In particular case of slowly varying curvatures the equation that describes the dynamics of the fluxion can be obtained in much faster way. In this regime the dynamics of the fluxion can be obtained by the dimensional reduction of the 3+1 dimensional sine-Gordon model to curved lower dimensional subspace identified with the Josephson junction.

In the next sections we use the differential geometry formalism that appears in description of many physical and biological systems [4, 9, 21, 22, 25–27, 31], in order to obtain the reduced models that describe the dynamics of the magnetic flux in the long and large area Josephson junctions.

2. Long Josephson Junction and its Possible Technical Applications

First we presume that the external bias current is absent in the system and we neglect the effects connected with the quasiparticle tunnelling ($\gamma = 0$) and a concomitant destruction and creation of pairs on different sides of the junction ($\beta = 0$). In case of slowly varying curvatures the effective model that describes the dynamics of the gauge invariant phase difference can be obtained by dimensional reduction of the 3+1 dimensional sine-Gordon model to 1+1 dimensions [8]. This procedure starts from the Lagrangian density

$$\mathcal{L} = \frac{1}{2}(\partial_t\phi)^2 - \frac{1}{2}\eta_E^{ij}(\partial_i\phi)(\partial_j\phi) - V(\phi) \tag{6}$$

where $V(\phi) = 1 - \cos\phi$ and $\eta_E^{ij} = \mathrm{diag}(+1, +1, +1)$ is Euclidean metric. Moreover we use dimensionless coordinates $x^i \to \frac{x^i}{\lambda_J}$ and $t \to \omega_P t$, where ω_P is plasma frequency. First we rewrite the second term of the Lagrangian density in curved coordinates defined in the neighborhood of the curve located in the central plane

$$\mathcal{L} = \frac{1}{2}(\partial_t\phi)^2 - \frac{1}{2}G^{\alpha\beta}(\partial_\alpha\phi)(\partial_\beta\phi) - V(\phi). \tag{7}$$

Here the curved coordinates consists of one coordinate that parameterizes the curve denoted by s and two normal coordinates to the curve ρ^j i.e. $\xi^\alpha = (\xi^1, \xi^2, \xi^3) = (s, \rho^1, \rho^2) = (s, \rho, u)$. The points on the curve are indicated by the vector field $\vec{X}(s)$. The coordinates are connected with the local frame that consists of tangent vector to the curve $\vec{t} = \vec{X}_{,\,s} \equiv \frac{\partial}{\partial s}\vec{X}$ and two normal vectors $(\vec{n}_j) = (\vec{n}_1, \vec{n}_2) = (\vec{n}, \vec{b})$. In fact, the first vector is normal to the curve and the second is binormal. Additionally, the normal vectors are normalized to unity

$$\vec{n}_i\vec{n}_j = \delta_{ij}, \qquad \vec{n}_j\vec{X}_{,s} = 0. \tag{8}$$

Because it was shown [8] that in case of long Josephson junctions the torsion has no impact on dynamics of the fluxion we consider torsion free curves. In case of plane curves Frenet - Serret formulas have the simple form:

$$\partial_s \vec{t} = \partial_s \vec{X}_{,s} = \vec{X}_{,ss} = K\vec{n}, \quad \partial_s \vec{n} = \vec{n}_{,s} = -K\vec{t}, \quad \partial_s \vec{b} = \vec{b}_{,s} = 0 \tag{9}$$

where $K(s)$ is a curvature of the curve. Having the implicit relation between Cartesian and curved coordinates

$$\vec{x} = \vec{X}(s) + \rho^j \vec{n}_j(s) \tag{10}$$

one can calculate the metric components defined in the neighborhood of the curve

$$G_{\alpha\beta} = \frac{\partial x^i}{\partial \xi^\alpha} \frac{\partial x^j}{\partial \xi^\beta} \eta^E_{ij}. \tag{11}$$

The components of this metric are the following

$$G_{ij} = \delta_{ij}, \qquad G_{is} = 0, \qquad G_{ss} = \mathcal{G}^2 = (1 - uK(s))^2. \tag{12}$$

The Lagrangian density in curved coordinates takes the form

$$\mathcal{L} = \frac{1}{2} (\partial_t \phi)^2 - \frac{1}{2G} (\partial_s \phi)^2 - V(\phi) \tag{13}$$

where we used the fact that the gauge invariant phase difference does not depend on the normal coordinates. Next, we integrate with respect to normal coordinates

$$L = \int \mathrm{d}s\mathrm{d}\rho\mathrm{d}u \sqrt{G}\, \mathcal{L} \tag{14}$$

and we obtain

$$L = \int \mathrm{d}s \mathcal{L}_{eff} \tag{15}$$

where the effective Lagrangian density has the form

$$\mathcal{L}_{eff} = \frac{1}{2} (\partial_t \phi)^2 - \frac{1}{2} \mathcal{F} (\partial_s \phi)^2 - V(\phi). \tag{16}$$

The clear picture of interaction of the fluxion with the curved region of the junction can be obtained in the framework of the collective coordinate method. In order to simplify the description we reduce the dynamics of the kink to the dynamics of the collective variable that describes the position $S(t)$ of the kink

$$\phi_K = 4 \arctan \left[\mathrm{e}^{s - S(t)} \right]. \tag{17}$$

The integration with respect to s variable leads to the effective mechanical Lagrangian for the $S(t)$ variable

$$L_{eff} \approx 4wb\dot{S}^2 - 8wb - \Delta U \tag{18}$$

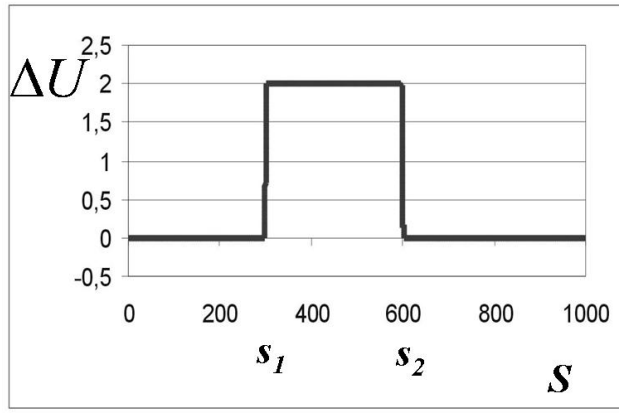

Figure 1. The potential experienced by the fluxion in the junction that consists of two straight segments $[0, s_1]$ and $[s_2, l = 1000]$ connected by the circular part $[s_1, s_2]$ has a form of the barrier.

where the constants w and b denote the widths of the dielectric layer in both normal directions. The explicit formula for potential can be obtained for small curvatures $K(s) << 1/w$

$$\Delta U \approx \frac{bw^3}{6} \int_0^l \mathrm{d}s \frac{K(s)^2}{\cosh^2(s-S)}. \tag{19}$$

For example, if we prepare the junction that consists of two flat sections connected by the arc of the circle then the potential experienced by the fluxion has a form of the barrier (see Fig. 1).

The Josephson junction finds application in RSFQ (rapid single flux quantum) electronics. RSFQ is digital electronics that uses fluxions as carriers of information. It was invented by Likharev and his collaborators [20], who have suggested new way of coding a digital information. The Josephson junctions in this technology are the active elements, similarly like transistors are the active elements for traditional semiconductor electronics. The fluxions that are magnetic flux quanta are carried by picosecond-duration voltage pulses which travel along the superconducting transmission lines. Moreover, depending on the particular parameters of the Josephson junction, the pulses can be even shorter than one picosecond with a low amplitude. The main advantage of such elements is extremely fast operating frequency reaching hundreds of gigahertz. In fact, digital RSFQ circuits working at frequencies close to THz were demonstrated by several groups [7,19]. Nevertheless, the operating clock frequencies of the middle-scale RSFQ systems are on the level of few tens GHz [6, 29]. The other advantage, in comparison with standard

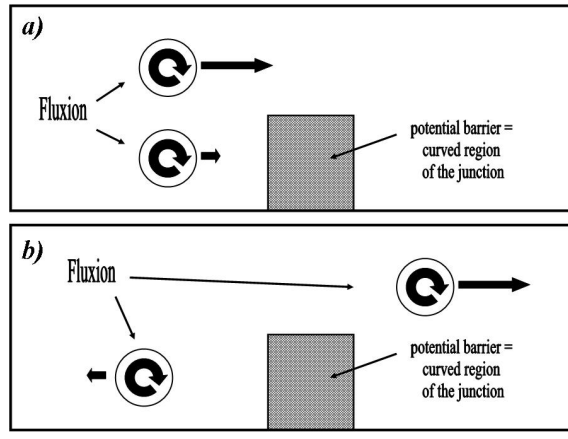

Figure 2. Fast and slow fluxion in the discriminating element a) before interaction with the curved region of the junction b) after interaction.

semiconductor technology, is extremely low power consumption. For example, the energy dissipated during one switching of a Josephson junction is of order 10^{-19} Joule.

A curvature of the Josephson junction can be used in RSFQ electronics in two ways. First, the junction with one curved region can act on fluxions in electronic circuits as discriminating element. In this element the sufficiently fast fluxions can pass through the curved region of the junction. At the same time the slow fluxions are reflected and start their movement in opposite direction. This element can be used in order to separate slow from fast fluxions (see Fig. 2). Second, application is connected with storage of a binary data in the form of fluxions. In this proposal the potential hole is formed between two curved regions of the junction. Essential for work of this element is existence of the quasiparticle current between the superconducting electrodes that introduces the small dissipation term to the equation of motion (1). As a consequence of this dissipation the fluxions with the speeds slightly exceeding the critical speed, necessary to overcome the first barrier, can be confined in the potential hole (located between two curved regions of the junction). Moreover, the reading out of the digital data can be achieved by application of the external bias current (see Fig. 3). Let us notice that efficiency of this trap depends on dissipation constant, the distance between curved regions and the heights of the barriers (in particular on the difference of these heights).

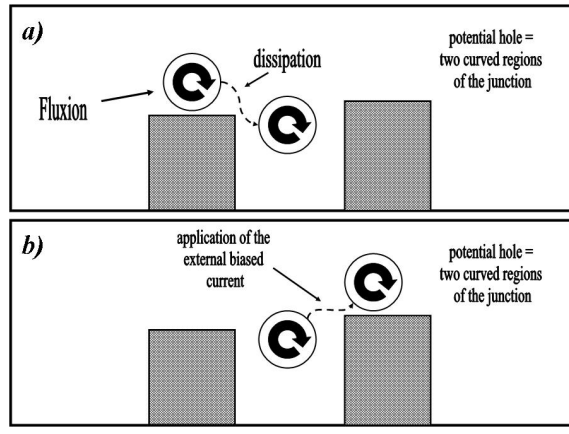

Figure 3. Storage of the digital data in the form of fluxions. a) Dissipation is responsible for confining the fluxions in the potential hole. b) The reading out of the digital data can be achieved by application of the external bias current.

3. Large-Area Josephson Junction

A procedure that works for slowly varying curvatures in 1+1 dimensions we could apply to 2+1 dimensional system [10, 11]. We start from Lagrangian density of the 3+1 dimensional sine-Gordon model

$$\mathcal{L} = \frac{1}{2}\eta_M^{\mu\nu}(\partial_\mu\phi)\,(\partial_\nu\phi) - V(\phi) \tag{20}$$

where $\eta_M^{\mu\nu} = \mathrm{diag}(+1,-1,-1,-1)$ is Minkowski metric and $(x^\mu) = (x^0,x^1,x^2,x^3) = (ct,x,y,z)$ are space-time coordinates. The potential has the standard form $V(\phi) = 1-\cos\phi$. Next, we separate space and time derivatives in Lagrangian density

$$\mathcal{L} = \frac{1}{2}(\partial_t\phi)^2 - \frac{1}{2}\eta_E^{ij}(\partial_i\phi)(\partial_j\phi) - V(\phi) \tag{21}$$

here $(x^i) = (x^1,x^2,x^3) = (x,y,z)$ are space variables and $\eta_E^{ij} = \mathrm{diag}(+1, +1,+1)$ is Euclidean metric. The same Lagrangian density in curved coordinates $(\xi^i) = (\xi^1,\xi^2,\xi^3) = (s,\sigma,\xi)$ defined in the neighborhood of the central surface of the junction take the form

$$\mathcal{L} = \frac{1}{2}(\partial_t\phi)^2 - \frac{1}{2}G^{ij}(\partial_i\phi)(\partial_j\phi) - V(\phi). \tag{22}$$

Let us notice that the first two coordinates $(\sigma^a) = (\sigma^1,\sigma^2) = (s,\sigma)$, parameterize the central surface. The last curved coordinate ξ parameterize the normal direction

to this surface. The points on the surface are indicated by the vector field $\vec{X} = \vec{X}(s,\sigma)$. The tangent vectors to the surface we denote as follows

$$\vec{X}_{,\,a} \equiv \partial_a \vec{X} \equiv \frac{\partial \vec{X}}{\partial \sigma^a}. \tag{23}$$

The tangent vectors define the metric induced on the central surface

$$g_{ab} = \vec{X}_{,\,a}.\vec{X}_{,\,b}. \tag{24}$$

The implicit relation between the Cartesian and curved coordinates

$$\vec{x} = \vec{X}(s,\sigma) + \xi \vec{n}(s,\sigma) \tag{25}$$

enables explicit calculation of the metric components in curved coordinates. Here $\vec{n}$ is a normal vector to the surface

$$\vec{n}.\vec{n} = 1, \qquad \vec{n}.\vec{X}_{,\,a} = 0. \tag{26}$$

The normal vector is normalized to unity. In calculus we use the Gauss - Weingarden formulas which describe the change of tangent and normal vectors under infinitesimal shift along the surface

$$\partial_a \vec{X}_{,\,b} = \vec{X}_{,\,ab} = \Gamma^c_{ab}\vec{X}_{,\,c} - K_{ab}\vec{n}, \qquad \partial_a \vec{n} = \vec{n}_{,\,a} = K^c_a \vec{X}_{,\,c}. \tag{27}$$

Here K_{ab} are external curvature components

$$K_{ab} \equiv -\vec{n}.\vec{X}_{,\,ab} \tag{28}$$

and Christoffel symbols Γ^c_{ab} are calculated with respect to the metric induced on the surface. The metric in curved coordinates has a form

$$G^{ij} = \begin{bmatrix} G^{ab} & 0 \\ 0 & 1 \end{bmatrix} \tag{29}$$

where

$$G^{ab} = \frac{1}{\mathcal{G}^2}\left[(1+\xi K^c_c)^2 g^{ab} - 2\xi(1+\xi K^c_c)K^{ab} + \xi^2 K^{ac}K^b_c\right] \tag{30}$$

and

$$\mathcal{G} = 1 + \xi K^a_a + \frac{1}{2}\,\xi^2 \mathcal{R}. \tag{31}$$

The curvature scalar $\mathcal{R}$ enters to the above formula through Gauss integrability condition. The effective 2+1 dimensional model is obtained by integration of the Lagrangian

$$L = \int_{-l/2}^{+l/2} \mathrm{d}s \int_{-b/2}^{+b/2} \mathrm{d}\sigma \int_{-w/2}^{+w/2} \mathrm{d}\xi \sqrt{G}\mathcal{L} \tag{32}$$

with respect to normal variable. The effective sine-Gordon theory on the curved surface is defined by the Lagrangian

$$L = \int_{-l/2}^{+l/2} \mathrm{d}s \int_{-b/2}^{+b/2} \mathrm{d}\sigma \sqrt{g} \mathcal{L}_2. \tag{33}$$

Here w denotes thickness of the dielectric layer. The effective Lagrangian density for this system is the following

$$\mathcal{L}_2 = \frac{1}{2}\mathcal{C}(\partial_t \phi)^2 - \frac{1}{2}\mathcal{M}^{ab}(\partial_a \phi)(\partial_b \phi) - \mathcal{C}\, V(\phi) \tag{34}$$

where we used the following abbreviations $\mathcal{C} = 1 + \frac{w^2}{24}\mathcal{R}$

$$\mathcal{M}^{ab} = \mathcal{A}\, g^{ab} + \mathcal{B}\, K^{ab} + \mathcal{D}\, K^{ac} K_c^b \tag{35}$$

and g is determinant of the metric induced on the surface. The quantities $\mathcal{A} = \mathcal{A}(K, \mathcal{R}, w)$, $\mathcal{B} = \mathcal{B}(K, \mathcal{R}, w)$ and $\mathcal{D} = \mathcal{D}(K, \mathcal{R}, w)$ are functions defined by the geometry of the system. The important property of this expression is the fact that the quantities $\mathcal{A}$, $\mathcal{B}$, $\mathcal{D}$ are scalars with respect to reparameterization of the central surface and therefore does not affect tensor structure of the symbol $\mathcal{M}^{ab}$. Here and in other formulas we make summation over repeated indices. For example, for small curvatures $K << 1/w$ this auxiliary symbol takes the form

$$\mathcal{M}^{ab} = (1 - \frac{w^2}{24}\mathcal{R}) g^{ab} + \frac{w^2}{12} K^{ac} K_c^b. \tag{36}$$

One could have a temptation to test some gravitational effects in this simple 2+1 dimensional system. In order to transform this model to gravitational form we define a new space-time metric tensor and moreover transform the Lagrangian density to its natural form.

4. Curved Josephson Junction - Gravitational Analogy

The curvature which determines the behavior of a scalar field in the junction suggests the possibility of using this system to simulate the behavior of a scalar field in a curved space-time with fixed background. In fact, despite appearances the system under consideration is more similar to 3+1 than to 2+1 gravity. This observation is related to the fact that, in two dimensions, the Weil tensor disappears identically. In fact the 2+1 gravity is significantly different from 3+1 gravity theory [15]. In 2+1 dimensions the Riemann curvature is solely defined by the Ricci tensor and therefore it is completely determined by the local matter distribution. As a consequence of this fact, for example, two separated point masses move uniformly and rectilinearly without local interaction. Moreover, even a cloud of dust exhibits no local interaction. As a matter of fact in 2+1 dimensions the space-time produced

by a point mass is locally flat although globally it has a conic structure. Additionally, there are no gravitational waves in 2+1 gravity. Finally, the Einstein equations in 2+1 dimensions, for slow motion and week fields, reduce to Laplace equation. This fact stands in contradiction to the Newtonian limit of the 3+1 gravity theory which is defined by the Poisson equation.

First we introduce the new space-time metric

$$(\mathbf{g}^{\alpha\beta}) = \begin{pmatrix} \mathbf{g}^{00} & 0 \\ 0 & \mathbf{g}^{ab} \end{pmatrix} \tag{37}$$

where $(\alpha) = (0, a) = (0, 1, 2)$. In order to identify the components of this new metric tensor we transform the Lagrangian as follows

$$L = \int_{-l/2}^{+l/2} \mathrm{d}s \int_{-b/2}^{+b/2} \mathrm{d}\sigma \sqrt{g}\mathcal{L}_2 = \int_{-l/2}^{+l/2} \mathrm{d}s \int_{-b/2}^{+b/2} \mathrm{d}\sigma \sqrt{\mathbf{g}}\tilde{\mathcal{L}}_2.$$

Although, we do not change Lagrangian as a whole we introduce a new Lagrangian density and a new metric. The crucial for this procedure is identification

$$\sqrt{g}\mathcal{L}_2 = \sqrt{\mathbf{g}}\tilde{\mathcal{L}}_2. \tag{38}$$

If we treat the dimensionless quantity

$$\varepsilon \equiv \frac{w^2}{24}\mathcal{R}$$

in formulas (34-36) as a small parameter then in zero order approximation we obtain the following components of the metric tensor

$$\mathbf{g}^{00} = 1, \qquad \mathbf{g}^{0a} = 0, \qquad \mathbf{g}^{ab} = -g^{ab} \tag{39}$$

where the space components of this tensor are solely determined by the metric induced on the central surface of the junction. Additionally, the effective Lagrangian density has a natural form

$$\tilde{\mathcal{L}}_2 = \frac{1}{2}\,\mathbf{g}^{\alpha\beta}(\partial_\alpha\phi)(\partial_\beta\phi) - V(\phi). \tag{40}$$

In the first order approximation the same quantities take the form

$$\mathbf{g}^{00} = 1 + \frac{w^2}{20}\left(\mathcal{R} - \frac{1}{3g}K^a{}_b K^b{}_a\right), \qquad \mathbf{g}^{0a} = 0 \tag{41}$$

$$\mathbf{g}^{ab} = -g^{ab} + \frac{w^2}{30}\,g^{ab}\left(\mathcal{R} + \frac{1}{2g}K^a{}_b K^b{}_a\right) - \frac{w^2}{12}K^{ac}K^b_c. \tag{42}$$

In the first order expansion the curvature scalar and the external curvatures enter into space components. We would like to underline that both the curvature scalar

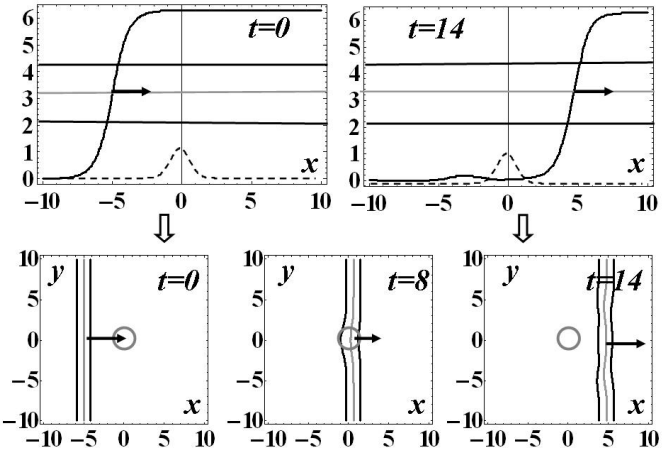

Figure 4. In the top figures the profiles of the gauge invariant phase difference ϕ is presented at instants $t = 0$ and $t = 15$. The gray line represents the center of the kink and the black lines corresponds to the two values $\pi + 2$,$\pi - 2$. The curved region is represented by the dashed line. In the bottom figures the curved region is denoted by the circle. We see contour lines that represent the kink front. Two black lines correspond to the values $\pi + 2, \pi - 2$ of the field ϕ and the position of the kink front is represented by the gray contour line π. We see that in the region of interaction the speed of the kink front is reduced and the thickness grows. After interaction the kink moves with the speed that is similar to the initial speed and the kink front becomes almost flat.

and the external curvatures, as the background is fixed, are defined by some known functions. This time the effective Lagrangian density is the following

$$\tilde{\mathcal{L}}_2 = \frac{1}{2}\,\mathbf{g}^{\alpha\beta}(\partial_\alpha\phi)(\partial_\beta\phi) - \widetilde{V}(\phi) \tag{43}$$

where the effective potential is modified by the curvature terms $\widetilde{V}(\phi)$

$$\widetilde{V}(\phi) = V(\phi) + \frac{w^2}{20}\left(\mathcal{R} - \frac{1}{3g}K^a{}_b K^b{}_a\right) V(\phi). \tag{44}$$

Finally, we consider an example of the background with circular symmetry. Moreover, the curvature of the central surface has a gaussian form and therefore is well located in the center of the junction. The numerical studies lead to the following description of the interaction of the kink front with the curved region of the junction. At the beginning the kink front moves almost freely in the direction of the curved region. Next, as a consequence of interaction the kink front with curvature

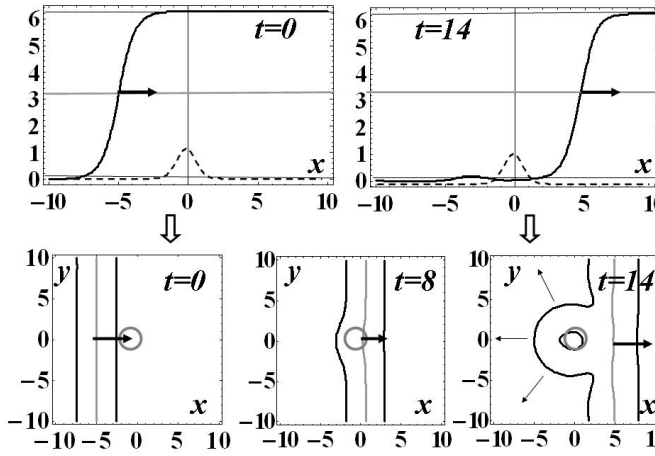

Figure 5. In the top figures the gray line represents the center of the kink and the black lines corresponds to the two values $\pi + 3$,$\pi - 3$. In the bottom figures two black lines correspond to the values $\pi + 3, \pi - 3$ of the field ϕ and the position of the kink front is represented by the gray contour line π. At an initial time the kink seems to be thicker but still it is the same field configuration as in figure 4. At the final instant of time the circular wave that propagates from the center of the curved region is created.

of the space we observe deformation which is a consequence of slowing down and widening of the front. Finally, when the curved area has been overrun, the front moves only with small deformation in the same direction (see Fig. 5). If we look for details of this interaction we can find out that during the interaction some circular waves are created which move in radial directions with respect to center of the curved region of the junction (see Fig. 4).

This process could bee seen as a visualization of the interaction of the domain wall (kink front) with the gravity center (curved region).

Acknowledgments

This work was supported in part by NCN Grant 2011/03/B/ST3/00448.

References

[1] Ablowitz M. and Clarkson P., *Solitons, Nonlinear Evolution Equations and Inverse Scattering*, Cambridge Univ. Press, Cambrige 1999.

[2] Anderson P. and Rowell J., *Probable Observation of the Josephson Superconducting Tunnelling Effect*, Phys. Rev. Lett. **10** (1963) 230–232.
[3] Arodź H., *Expansion in the Width and Collective Dynamics of a Domain Wall*, Nucl. Phys. B **509** (1998) 273-293.
[4] Aulisa E., Ibraguimov A. and Toda M., *Geometric Methods in the Analysis of Non-Linear Flows in Porous Media*, Contemporary Mathematics Proceedings of the AMS, *Spectral Theory and Geometric Analysis*, in honor of M. Shubin, L. Friedlander (Ed), **535** (2011) 27-42.
[5] Barone A. and Paterno G., *Physics and Applications of the Josephson Effect*, Wiley, New York, 1982.
[6] Bunyk P., Leung M., Spargo J. and Dorojevets M., *FLUX-1 RSFQ Microprocessor*: *Physical Design and Test Results*, IEEE T. Appl. Supercon. **13** (2003) 433–436.
[7] Chen W., Rylyakov A., Patel V., Lukens J. and Likharev K., *Rapid Single Flux Quantum T-Flip Flop Operating up to 770 GHz*, IEEE T. Appl. Supercon. **9** (1999) 3212–3215.
[8] Dobrowolski T., *Kink Motion in a Curved Josephson Junction*, Phys. Rev. E **79** (2009) 046601–1–7.
[9] Dobrowolski T., *Geometry of Minimally Deformed Vortices and Domain Walls*, J. Geom. Symmetry Phys. **22** (2011) 1–12.
[10] Dobrowolski T., *The Dynamics of the Kink in Curved Large Area Josephson Junction*, DCDS-S **4** (2011) 1095–1105.
[11] Dobrowolski T., *The Studies on the Motion of the Sine-Gordon Kink on a Curved Surface*, Ann. Phys. (Berlin) **522** (2010) 574–583.
[12] Dobrowolski T., *Curved Josephson Junction*, Ann. Phys. (N.Y.) **327** (2012) 1336–1354.
[13] Dobrowolski T., *The Fluxion in a Curved Josephson Junction*, J. Geom. Symmetry Phys. **34** (2014) 13–26.
[14] Ferreira L., Piette B. and Zakrzewski W., *Wobbles and Other Kink-Breather Solutions of the Sine-Gordon Model*, Phys. Rev. E **77** (2008) 036613–1–9.
[15] Giddings S., Abbott J. and Kuchar K., *Einstein's Theory in a Three-Dimensional Space-Time*, Gen. Relat. Gravit. **16** (1984) 751–775.
[16] Ivancevic V. and Ivancevic T., *Sine–Gordon Solitons, Kinks and Breathers as Physical Models of Nonlinear Excitations in Living Cellular Structures*, J. Geom. Symmetry Phys. **31** (2013) 1–56.
[17] Josephson B., *Possible New Effects in Superconductive Tunnelling*, Phys. Lett. **1** (1962) 251–253.
[18] Josephson B., *Supercurrents Through Barriers*, Adv. Phys. **14** (1965) 419–451.
[19] Kaplunenko V., Khabipov M., Koshelets V., Likharev K., Mukhanov O., Semenov V., Serpuchenko I. and Vystavkin A., *Experimental Study of the RSFQ Logic Elements*, IEEE T. Magn. **25** (1989) 861–864.
[20] Likharev K., Mukhanov O. and Semenov V., *Resistive Single Flux Quantum Logic for the Josephson-Junction Technology*, SQUID'85 (1985) 1103–1108.
[21] Marinov P. and Mladenov I., *A Relation Between the Cylindric Fluid Membranes and the Motions of Planar Curves*, J. Geom. Symmetry Phys. **27** (2012) 93–102.
[22] Ogawa N., *Curvature-Dependent Diffusion Flow on a Surface with Thickness*, Phys. Rev. E **81** (2010) 061113–1–8.

[23] Parmentier R., *Fluxons in Long Josephson Junctions*, in *Solitons in Action*, Lonngren K. and Scott A. (Eds), Academic Press, New York 1978.
[24] Pederson N., *Solitons in Josephson Transmission Lines*, In *Solitons*, S.E. Trullinger et al (Eds), Elsevier, Amsterdam 1986.
[25] Pulov V. and Chakarov E., *Cylindrical Shapes of Helfrich Spontaneous-Curvature Model*, J. Geom. Symmetry Phys. **36** (2014) 99–115.
[26] Rożko E.-E., *Quantization of Affinely Rigid Bodies with Degenerate Dimension*, Rep. Math. Phys. **65** (2010) 1–15.
[27] Sławianowski J. J., Kovalchuk V., Gołubowska B., Martens A. and Rożko E.-E., *Quantized Excitations of Internal Affine Modes and Their Influence on Raman Spectra*, Acta Phys. Pol. B **41** (2010) 165–218.
[28] Swihart J., *Field Solution for a Thin-Film Superconducting Strip Transmission Line*, J. Appl. Phys. **32** (1961) 461–469.
[29] Tanaka M., Yamanashi Y., Irie N., Park H.-J., Iwasaki S., Takagi K., Taketomi K., Fujimaki A., Yoshikawa N., Terai H. and Yorozu S., *Design and Implementation of a Pipelined 8 Bitserial Single-Flux-Quantum Microprocessor with Cache Memories*, Supercond. Sci. Tech. **20** (2007) S305-S309.
[30] Toda M., *Initial Value Problems of the Sine-Gordon Equation and Geometric Solutions*, math/0307270v2.
[31] Trzęsowski A., *On the Isothermal Geometry of Corrugated Graphene Sheets*, J. Geom. Symmetry Phys. **36** (2014) 1–45.